Interpreting Emergent Features in Deep Learning-based Side-channel Analysis

Sengim Karayalçin
Leiden University, The Netherlands
s.karayalcin@liacs.leidenuniv.nl

Marina Krček
Radboud University, The Netherlands
marina.krcek@ru.nl

Stjepan Picek
Univ. of Zagreb Faculty of Elec. Eng. and Computing, Unska 3, 10000, Zagreb, Croatia &
Radboud University, The Netherlands
stjepan.picek@ru.nl

Abstract

Side-channel analysis (SCA) poses a real-world threat by exploiting unintentional physical signals to extract secret information from secure devices. Evaluation labs also use the same techniques to certify device security. In recent years, deep learning has emerged as a prominent method for SCA, achieving state-of-the-art attack performance at the cost of interpretability. Understanding how neural networks extract secrets is crucial for security evaluators aiming to defend against such attacks, as only by understanding the attack can one propose better countermeasures.

In this work, we apply mechanistic interpretability to neural networks trained for SCA, revealing *how* models exploit *what* leakage in side-channel traces. We focus on sudden jumps in performance to reverse engineer learned representations, ultimately recovering secret masks and moving the evaluation process from black-box to white-box. Our results show that mechanistic interpretability can scale to realistic SCA settings, even when relevant inputs are sparse, model accuracies are low, and side-channel protections prevent standard input interventions.

1 Introduction

Side-channel analysis (SCA) is a realistic security threat that consists of diverse methods that allow for the extraction and exploitation of unintentionally observable information of internally processed data [23]. SCA enables the establishment of a relationship between passively observable information and the internal state of a device under investigation. As such, it poses a major threat to devices that handle sensitive data like keys, private certificates, or intellectual property (see, e.g., [40, 41]). In SCA, sensitive information gets extracted from a device by observing its physical characteristics during computation (e.g., power consumption, timing).

Since 2016 [25], deep learning-based side-channel analysis (DLSCA) has received significant attention from the research community [36]. The main benefits of using deep learning (DL) over classical techniques are that assumptions about attacker capabilities can be relaxed, leading to better attack performance. Thus, integration of these techniques into evaluation procedures for cryptographic implementations has become standardized [12].

One of the main open challenges for black-box evaluations using DL is interpretability [36]. A model that can extract the key confirms there is some exploitable leakage, but does not indicate *how* the network exploits *what* leakage. Notably, this does not allow the evaluator to provide any feedback

39th Conference on Neural Information Processing Systems (NeurIPS 2025).

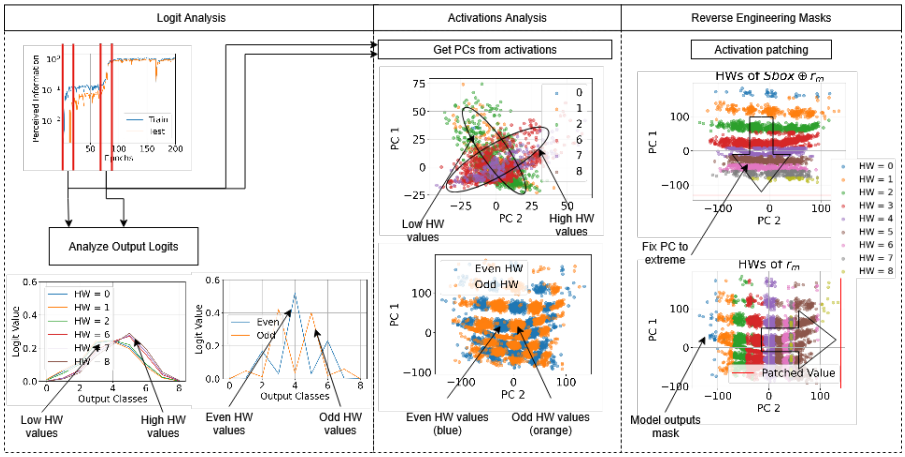

Figure 1: The analysis approach used in this study broadly consists of three major steps. After the performance increases are located using the PI metric, we plot logits to extract relevant features. Using these features, we plot the PCs of the activations and find the structure related to the leakage. Finally, we apply activation patching to reverse-engineer the masks.

beyond pass/fail, which complicates the cost-effective implementation of a solution. Understanding how neural networks learn to exploit side-channel information can prove crucial for developing robust defenses against these attacks [39]. Thus, several attempts have been made to understand network behavior. However, these approaches either focus only on input visualization [26, 18], use more explainable model architectures [52, 53], or require access to masking randomness [54, 35]. We discuss this related work in Appendix A.

Although interpreting how neural networks perform computations is generally difficult, the algorithmic tasks performed in models trained on side-channel data are conceptually relatively simple. Learning to extract leakage information from masked implementations is similar to toy models that learn group operations in the works on grokking [37, 30, 7, 56]. Concretely, for masked implementations, the computations on a sensitive value s are split into d secret shares $s = s_1 \cdot s_2 \cdots s_d$. Then, to learn to extract leakage from side-channel signals, a neural network needs to combine leakage from each of these shares, often without the knowledge of individual shares even for the training set [27].

The connection between side-channel and grokking models is further motivated by the observation of Masure et al. that the learning curves for models trained against masked targets show an 'initial plateau' (Section 5.2 of [27]). After a number of training steps where test loss does not improve, the models suddenly generalize to the test set and can extract the (sub)key. These sudden increases in performance raise the question of what the model is learning. Indeed, as some models for neural scaling predict neural networks learn in discrete steps [28], we expect that investigating what is learned during these transitions will give a reasonable understanding of model behavior. Recent successful results of mechanistic interpretability (MI) investigating sudden generalization[1] in toy models [30, 42] and even language models [33] further motivate this direction.

From the point of view of MI, side-channel data provides an interesting test case. The data is often noisy, high-dimensional, characterized by subtle dependencies that are difficult to capture and interpret, and presents a real-world scenario. Additionally, the masks are hidden values and should not be publicly accessible[2] which further complicates the application of MI as we cannot describe model behavior exhaustively with respect to concrete input features as in [30, 7], or do (automated) input interventions to align with a causal model as in [14, 8].

In this work, we aim to understand **what specific side-channel leakage a successful network has learned to exploit**. Concretely, we derive features from model outputs, find geometric structures that emerge in principal components (PCs) during sudden jumps in performance (phase transitions), and relate these to the physical leakage. As a practical consequence, we utilize this emergent structure to

[1] Sometimes referred to as phase transitions in related works [30, 33].

[2] Even in evaluation contexts with collaboration from developers, this is often impossible; see the introduction of [27] for an in-depth discussion.

extract input features, i.e., individual shares s_i related to device internal randomness, from model activations, providing a path to move from black-box to white-box evaluations. The overall analysis process is illustrated in Figure 1.

To summarize, our main contributions are:

- We explore the feasibility of applying MI in a challenging real-world setting where input interventions to features are not possible due to SCA countermeasures.
- By investigating the changes in model outputs during sudden jumps in model performance, we find how networks combine leakage in DLSCA.
- We directly retrieve the internal secret share values by applying activation patches[3] to intermediate layer activations across several targets.
- We provide more detailed insights into the specific physical leakage that neural networks exploit for widely used (DL)SCA benchmark datasets. Notably, we do this without assuming a priori mask knowledge [54, 35] or requiring custom architectures [52, 53].
- We find identical structures emerging during sudden generalizations for models trained on side-channel traces captured on different implementations and in different SCA domains (electromagnetic vs. power), providing further evidence for the weak universality hypothesis [7].

Code to reproduce experiments is available at `https://github.com/Sengim/feature_emergence`.

2 Background

Deep learning-based SCA (DLSCA): The main principle behind SCA is that during the execution of an algorithm on a physical device, side-channel information, e.g., power or electromagnetic (EM) measurements, can be influenced by secret-dependent internal computation [23]. For example, under standard assumptions, writing 0000 to a register will consume less power than 1111. The goal of SCA is then to extract this secret from the side-channel observations to establish security bounds for devices that operate in conditions where physical access may be possible for attackers (e.g., bank cards, passports, mobile phones). While many SCA variants exist, a common division is into direct and profiling attacks [36]. Direct attacks assume a single device where the attacker uses (classical) statistical techniques to find the most likely key.

In profiled attacks, which are often used by device evaluation labs [6], one assumes the attacker can access a copy of the device to be attacked. This copy is under the complete control of the attacker and is used to build a model of the device. The attacker uses that model to attack a different (but similar) device. While profiled attacks are less practical due to the assumption of access to a copy of a device, it can be significantly more powerful than direct attacks. Indeed, provided that the model is well-built and there is sufficient information in the trace, one could need only a single trace from the device under attack to obtain the secret key. On the other hand, direct attacks may require significantly more traces to break a real-world target [36].One can easily observe a similarity between profiled attacks and the supervised machine learning paradigm (where building a model is training, and the attack is testing). Consequently, in the last decade and more, many machine (deep) learning algorithms have been tested in SCA [36].

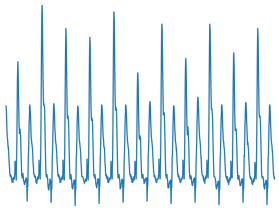

Figure 2: Example of a single trace captured during the execution of the Advanced Encryption Standard (AES) cipher [9].

The main workflow for SCA is to take a (large) number of traces (see Figure 2 for an example) from the profiling device with known key(s). These traces, often containing anywhere from 100-10 000 points per trace[4], are then labeled using an intermediate value used during the computation that

[3] Activation patching is a technique from MI.

[4] Generally, only a small number of points in the trace contains relevant information as the intermediate value is only used during few instructions, complicating classical SCA techniques.

depends on some public input (i.e., plaintext) and some sensitive data (i.e., the secret key). The exact mapping between the trace and intermediate values also depends on the assumed leakage model. An evaluator can employ Identity (ID) leakage model, which takes the intermediate values directly, or use leakage models that assume some physical leakage function, e.g., Hamming Weight (HW) or bitwise models. The chosen leakage model then also directly influences the number of labels (e.g., when working with a byte-oriented cipher like AES, the HW leakage model results in 9 classes, while the ID leakage model results in 256 classes). For AES, the label is often the output of the `S-Box` in the first round ($\texttt{S-Box}[p \oplus k]$) since it only depends on one plaintext and key byte (p and k). The neural network is then directly trained on these labeled traces, eliminating the need for labor-intensive (and often error-prone) feature engineering processes [36].

In the attack phase, the trained model is used to predict intermediate values from the traces of the target device. As models often have accuracies that are only marginally above random guessing, evaluating success is done by accumulating the predictions across a larger number of traces and evaluating which of the hypothetical key candidates[5] is the most likely. In evaluation settings, the model is then said to 'break' the device if the correct key is the top candidate within some specified number of traces [44]. Other information-theoretic metrics aim to directly quantify the secret information present in a single trace. Perceived Information (PI) [38], an easier-to-estimate lower bound on mutual information, is often used in DLSCA settings. Intuitively, a PI of 0.5 means there are 0.5 bits of key-related leakage in a single trace.

To protect against SCA, countermeasures such as hiding or masking are commonly used. In both cases, the goal is to remove the correlation between the observed quantity (traces) and secret information. Hiding countermeasures can happen in the amplitude domain by randomizing/smoothing the signal or by adding desynchronization/random delays in the time domain. Masking [20], on the other hand, divides a secret variable into several shares such that one needs to know all the shares to obtain the secret information. For instance, consider a Boolean masking of a secret variable s. If we combine that secret variable with a random value m, we obtain a new variable y: $y = s \oplus m$. Then, to obtain information about s, one needs to know both y and m. DLSCA can often automatically circumvent these countermeasures and still result in extremely efficient attacks without requiring additional access assumptions (e.g., the ability to disable countermeasures on the copy device). For a practical introduction to DLSCA, we refer readers to [22], and for a broader overview of SCA, see [43].

Mechanistic Interpretability: Mechanistic interpretability (MI) aims to reverse engineer a neural network into human-understandable algorithms [32, 31, 48, 30]. This involves identifying "features", which are directions in internal representations that correspond to concepts, and "circuits", which are subgraphs within the network composed of interconnected neurons and their weights, representing meaningful computations. Generally, the first step in the process of MI is to identify the features. Examples of features include low-level features such as curve or edge detector neurons in vision models [32], or more high-level features corresponding to the board state in toy models trained on board games [24, 29]. As features generally correspond to linear directions in the latent space, training linear probes [1], i.e., small classifiers, is common for showing the presence of features in the latent space.
After finding features, the goal becomes to determine how these features relate to model outputs (or other features). Ideally, we can create a causal abstraction of network behavior based on feature descriptions [14]. One method for showing causal effects involves intervening in model activations by performing activation patches [17]. Here, we replace (part of the) activations during a forward pass with saved activations from another forward pass corresponding to a different feature value to understand the effects on model outputs. This allows for measuring the impact of a specific feature or, eventually, verifying that the circuit is a (faithful) description of the model behavior.

3 Analysis Approach

The analysis process is shown in Figure 1 and detailed in this section. However, additional analysis and MI techniques might have been used depending on the observed behavior and findings of each specific dataset. These additional steps and the reasons for them will be described directly in the experimental results (Section 4).

[5] As we target a byte at a time, exhaustively searching over 256 values is easy.

Assumptions. In (DL)SCA, the attack typically focuses on extracting a subkey (often a single key byte) of the secret key. As we target post-hoc analysis of successful models, our analysis assumes that the attack has already succeeded and the subkey has been recovered. This assumption allows us to label (test) traces by deriving the intermediate value (label) from the input (plaintext) and the key (recall that we target `S-box`$[p \oplus k]$). We do not assume we have access to mask values. **The goal is to understand the model's behavior and identify what information it extracts from the traces to make predictions.** Additionally, we aim to recover the masks used in the cryptographic algorithm, which enables us to recover the rest of the secret key with (significantly) less effort. Note that when the model fails to recover the correct subkey, suggesting that the underlying masks and feature representations were not properly learned, interpretability methods offer limited insight.

Logit Analysis. Once we have a model that successfully recovers a subkey, our primary goal during initial exploratory testing is to understand the factors influencing the network's predictions. To achieve this, we analyze models at points directly after generalization and observe changes in the model predictions. As these sudden changes in performance suggest significant changes in the neural network's behavior during training, they are shown to be useful for discerning features [56]. We examine the distributions of output logits for different classes, looking for clear separations between classes, indicating distinct patterns in the traces. We aggregate the distribution for model outputs for traces that belong to each class and visualize them to identify commonly confused classes. These insights enable us to formulate hypotheses about higher-level features influencing predictions. Opposed to other recent works that reverse engineer models, see, e.g., [30, 48], where the authors assign features to (or derive features from) model inputs, we rely on output logits as we do not have access to masking randomness. Additionally, the (physical) noise inherent to side-channel traces results in final model accuracies that can be only marginally above random guessing, making single trace predictions challenging to analyze from the MI perspective. Note that the analysis becomes easier in white-box SCA settings, where one would assume knowledge of all internal values during computation, including the masking randomness, see [35].

Activations Analysis. After finding and testing initial hypotheses about the physical leakage used for classification, we can look at activations and how these relate to the predictions. Considering that in SCA only a small number of operations in each trace should be relevant for the classification (i.e., only leakage related to the target value), the number of relevant features should be relatively small. This means PCA will likely reveal the features the model learns during the first phase transitions [42, 56]. Note that for more complicated tasks where there are more features than dimensions, sparse autoencoders can be an alternative to extract features [10, 4].

As we expect structure to emerge in the first few PCs [42], we can plot the distribution of attack traces for features we derive from the logit analysis. Still, while we expect a specific structure would emerge in the first few PCs, some manual effort in determining the correct (number of) components and subdivisions might be necessary. However, in the tested cases, we notice the structure generally emerges with up to the first four components. Ideally, we see clear divisions between groups of traces belonging to certain values. Even if this is not the case due to noise, some regions might contain more/less of certain groups, and the overall distribution should be tied to (noisy) physical leakage. After finding some structure, we should explain how it arises in terms of the physical leakage that is in the trace. For example, if there is a grid-like structure in the PCs, we could assume that (embeddings of) two secret shares correspond to the $x - y$ directions of the grid since we have two shares.[6]

Reverse engineering masks with activation patching. When a structure is found, we need to verify that the hypothesized behavior is causally related to the model predictions in the expected way. We do this by fixing the directions that correspond to all but one share to a fixed value.
If possible, we try to fix them to 0 or some other value that allows easy descriptions of the output based on the one varying share. Then, we observe how the model outputs relate to the final share. If the hypothesis about model behavior is correct, we can also directly derive the values for a secret share from these patched outputs. Finally, after deriving secret shares, we can use Signal-to-Noise Ratio (SNR)[7] to plot where in the trace these shares leak to derive which secret share is which, i.e., which of the two shares is the mask and which the masked `S-box` output. Note that this patching

[6] For higher d, the structure will be in higher dimensions.

[7] SNR measures the signal variance versus the noise variance. In SCA, a higher SNR indicates a stronger signal compared to noise, making it easier to extract sensitive information.

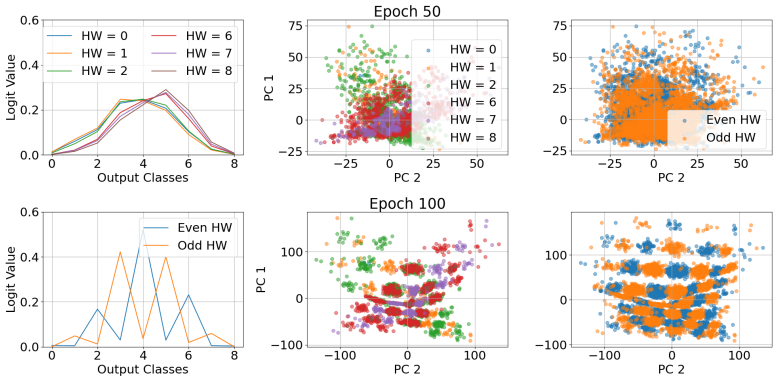

Figure 3: Logit analysis (first column) and activation analysis (remaining columns) from models at epoch 50 (top) and epoch 100 (bottom) for CHES_CTF. Legends for activation analysis are shared within columns. The difference in the number of points between the last two columns is due to not plotting the points for classes (HWs) 3, 4, and 5.

setup follows the activation patching method used in [35] without requiring a priori knowledge of secret share values.

4 Experimental Results

This section presents results for three common public SCA targets - CHES_CTF, ESHARD, and ASCAD (see Appendix B for details). The models are Multilayer Perceptron (MLP) neural networks with their hyperparameters taken from [35] for ESHARD and ASCAD (see Appendix C). For CHES_CTF, we directly train the ESHARD model without additional hyperparameter tuning. Note that we focus on MLP and CNN architectures as these are generally sufficient for state-of-the-art performance in SCA [34]. The analyses given here are similar (although somewhat more cumbersome) for CNNs (see Appendix G).

4.1 CHES_CTF Dataset

For the CHES_CTF target, we see in Figure 4 that there are two concrete increases in perceived information during training. The initial increase starts at epoch 15 and is completed around epoch 40. After another plateau in PI, there is a second increase between epochs 70-85, after which there are no more significant changes in PI.

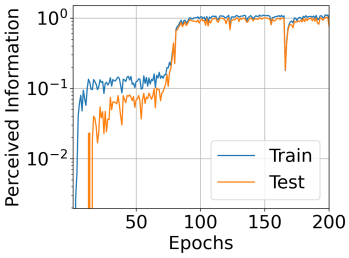

Figure 4: Evolution of Perceived Information for training and test traces of the CHES_CTF dataset.

As we aim to find what is learned during these performance jumps, we show both average logits for different classes and the two main PCs in Figure 3. After the first increase, at epoch 50, the predictions on the test set differentiate between high HW values and low HW values. When we use this information to plot PCs in the first layer (middle plot in Figure 3), we see that one diagonal corresponds to high HWs and the other to low HWs. This indicates that the HWs of both secret shares mask and masked `S-box` output leak in the HW leakage model and that these are the features that map onto the PCs. Further details are in Appendix H.

Looking at the logits after the second performance increase at epoch 100, Figure 3 shows that in addition to the high-low HW divide, the models also separate even-odd HWs. Plotting the same components but separating even-odd HWs shows a grid structure of even and odd points. In this grid, the number of changes in even-odd is about nine, corresponding to the nine possible HW values. The even-odd separation also clearly corresponds to learning the parity of a target value from HWs

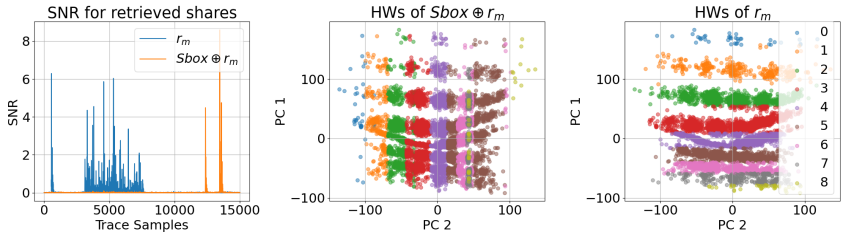

Figure 5: SNR plot and PC distributions for mask values using patching experiments for CHES_CTF. We set PC0 to -20 for both patching experiments, as that resulted in more apparent separation during manual testing.

with Boolean masking (see Appendix H.2). This leads to the ability to learn the mask values that the network uses for classification, as discussed next.

Activation Patching: To validate that the PC embeddings are causally related to model outputs, we can fix one of the components and observe the effects on model outputs. An additional consideration is that when we fix the value of one of the Hamming weights to 0 (or 8), the output of the model should be the HW value of the other share (or 8-output if we fix the first to 8).[8] As such, if the PCs relate to mask values, we can patch one share to 0 (or 8) to retrieve the value of the other share.

To practically extract mask values, we fix the value of one PC to be (near) one of the corners of the grid we see in Figure 3. Then, we examine the model outputs to verify whether the predicted value has changed as expected. As the model generally predicts HW values between 3-5 (because those occur most), we sort each trace by the difference of logits for high (5-8) and low (0-3) HWs. Since we know the expected number of occurrences for each HW[9], we can take the first 1/256 values to be $HW = 0$, then the next 8/256 values for $HW = 1$, and so on.

The resulting mask and masked `S-box` distribution are shown in Figure 5. We can see that fixing values of certain PCs to extremes results in the model basing its predictions mainly on the other PC, as is expected when one of the shares is fixed to 0 (or 8). When we visualize the SNR for each share, we observe clear spikes corresponding to the usage of the leaking values. First, we see spikes related to the value of r_m, indicating the loading of the mask and some pre-processing before the encryption. Then later, we see leakage related to $\texttt{S-box}[p_i \oplus k_i] \oplus r_m$. Due to the page limit, ESHARD results are in the Appendix E. In summary, there is only one generalization spike, which results in the ability of the model to distinguish high-low HWs. The results are qualitatively the same as for CHES_CTF.

4.2 ASCAD Dataset

For the ASCAD target (the main benchmark for DLSCA research since its introduction in 2018 [2]), generally the ID leakage model is used as this results in better attack performance [2, 34]. As such, for this dataset, we additionally train linear probes for each bit of both the `S-box` input and output.

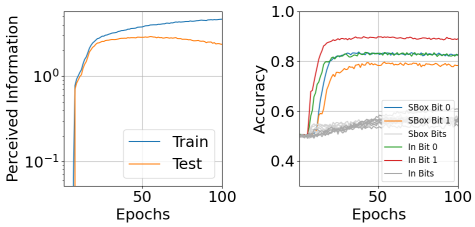

Figure 6: Evolution of PI and probe accuracies for bits during training for the ASCAD dataset.

Figure 6 shows a sudden transition to positive PI from epochs 8-12, corresponding to increased probe accuracies for the input bits. Immediately after, PI still increases marginally until improvement stops at epoch 25. This increase is accompanied by the increasing probe accuracies for the two least significant `S-box` output bits.

[8] Note that patching one share to be 0 to validate that the outputs become directly related to the other share has been done before in [35] although by using knowledge of the masking randomness.

[9] If the mask values are uniformly distributed, which they generally are for the security properties to hold [20].

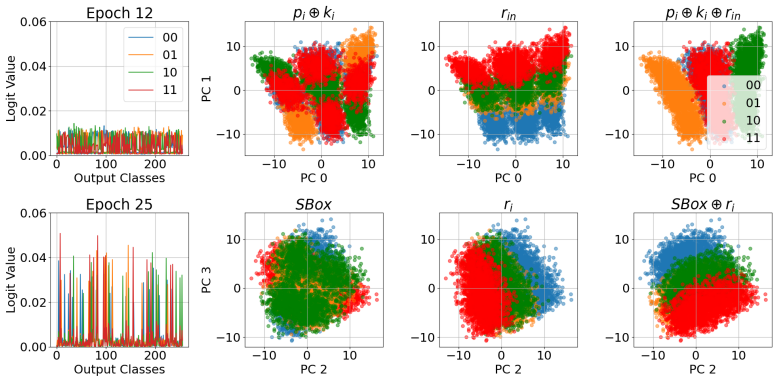

Figure 7: Logit analysis for two LSBs of $p_i \oplus k_i$ at epoch 12 and $\texttt{S-box}[p_i \oplus k_i]$ at epoch 25 with corresponding actual mask values for ASCAD. Note that for the lower logit plot, we use only traces with $p_i \oplus k_i$ in 00 for clarity, and that extracted mask values are in Figure 12.

Indeed, the two least significant bits (LSBs) for both input and output clearly achieve far higher accuracies than the other bits, which only marginally improve over random guessing.

Looking at the logits in Figure 7, at epoch 12, the values are distributed according to the two input bits. When we plot PCs to distinguish the values of these bits in Figure 7, we see an emerging structure in the first two PCs of the activations in the second layer corresponding to the combination of mask values by mapping these on certain axes. Note that the grid structure in both cases follows a 3×3 structure over the more ideal 4×4 if all four possible 2-bit values of the masks are perfectly distinguished. This is due to the physical leakage of two classes for the secret shares (mostly) overlapping, as shown in the two rightmost plots.

When we consider the logits at epoch 25 for the output bits,[10] the mean values are significantly higher. Additionally, the logits are spread out across fewer values. This aligns with the network's predictions, which now incorporate the information on the output bits. We also observe a visually similar structure to the grid at epoch 12 appearing in the 3rd and 4th PCs for the `S-box` output bits. The first two PCs remain related to the input bits as in epoch 12. Within the activation patching experiments for ASCAD, we observe causal effects on outputs by training probes on the final layer and selectively intervening on key components. However, further refinement is needed to extract mask values accurately. The experiments are presented in Appendix F.

5 Discussion

Recently, several works have characterized the algorithms learned by networks trained on simple algorithmic tasks, e.g., modular arithmetic and more general group operations [30, 7, 56]. Furthermore, other studies have identified individual circuits that perform grammatical operations in language models [48, 33]. These works showcase that interpretable algorithms are learned during discrete phase transitions, aligned with the neural scaling law from [28], which states that network training is a collection of discrete 'quanta' that correspond to (potentially interpretable) circuits. The eventual goal of interpreting a neural network then becomes to enumerate all of the phase transitions during training. In this work, we showcase that this type of ambitious interpretability can be possible for models trained on real-world datasets in SCA.

While this is a positive result, the broader relevance of this is somewhat limited. As mentioned in the introduction, side-channel data poses challenges due to noise and unpredictable physical leakage characteristics, but it is also very structured, and the number of relevant features is (expected to be) very low. The core task of the networks for SCA, combining secret share leakage to recover the target intermediate value, is very similar to the group operations learned in [30]. Indeed, in the networks we investigate, there are at most two jumps in performance, allowing for more detailed examination

[10] We fix the input bits to 00 to increase visibility, for a complete description, see Appendix I.1.

of each individual case. Additionally, the low number of expected features avoids issues that are prevalent in larger models trained on more general tasks (e.g., superposition [10]).

A key difference between our approach and those in previous works on group operations is that we assume no knowledge of input features due to our threat model. This then prohibits the use of standard input interventions, as we cannot replace input features. As such, we need to derive features from the model outputs and find which inputs are grouped together by the model. By finding these groups, we can work backwards from the model outputs to find relevant input features. This still requires domain-specific knowledge as, otherwise, it might not be immediately obvious that the grid structure in Figure 3 relates to the embedding of secret share HWs.

Another consideration is that our analysis is focused on model activations and outputs. We do not use other available information, like gradients or input visualizations, in this work. Some previous works have focused on visualizing what parts of the input the network is using (see Appendix A for some examples). However, without access to masking randomness, it is difficult to relate this to which shares and intermediate values are (not) being exploited. In contrast, the extraction of secret shares from model activations allows us to generate SNR graphs that match the visualizations in Figure 8 while splitting the individual shares. For automating analyses, gradient information could potentially be used, e.g., to identify phase transitions during training.

One of the most interesting points in our results is that the second performance jump in the CHES_CTF model seems to rely on the first. The high-low HW embeddings of the secret-share features gets progressively refined to be a direct embedding of the HW. When these embeddings are sufficiently clean, the model can distinguish even-odd HWs, as described in Appendix H.2. This indicates that adapting SCA training methodologies to first identify 'simpler' leakage and then build upon it with more complex leakage models could be a promising future direction for making models more efficient.

6 Relevance To DLSCA

As DLSCA becomes more common, it is increasingly important to understand how neural networks exploit implementations. This work provides concrete analyses for several common side-channel datasets, showing the possibility of reverse engineering masks from network activations. We show that specific structures can occur for different side-channel targets, indicating that building a library of common structures could be useful in analyzing future networks. This is especially relevant as masking schemes are often similar across ciphers (i.e., post-quantum ciphers often also use Boolean masking). As networks are often trained to recombine shares, these structures should be shared across different ciphers.

As our main practical result, we can reverse engineer secret shares from a trace by using the structures learned by the neural networks. To our knowledge, only [13] can extract mask values, where this work is focused on a specific implementation using classical side-channel techniques (thus, without considering machine learning approaches), which requires stronger assumptions than DL-based attacks. Extracting mask values substantially benefits evaluations, as we can move from black-box to white-box evaluations. This, in turn, would allow for better feedback to designers of cryptographic implementations.

One might question whether this is relevant for attackers, as we require a model that already breaks (one key byte of) the target. When attacks target individual bytes, the difficulty of breaking any individual byte can vary, even for the same device. As such, when masks are shared for all bytes (which is often required for masking non-linear operations, e.g., the `S-box` in AES), spending significant effort to break one key byte might allow retrieving the shared mask. Subsequent attacks against other key bytes become more straightforward as we can use the retrieved mask during training to effectively move the attack to an unprotected case by including the mask, see the white-box evaluations in [5].

Finally, discovering how neural networks concretely defeat countermeasures can improve evaluation/attack methodologies and countermeasure design. On the evaluation/attack side, we can design more effective methods for label distribution that consider common mistakes networks make, which can improve convergence [50]. On the defense side, understanding what type of leakage is more/less easily exploited could lead to the design of more (cost-)effective countermeasures that enable more

robust protections. Concretely, for the Boolean masking schemes we consider in this work, the structures that arise from the model embeddings of the secret share leakages into PCs naturally form the high-low structure. Further, when these embeddings are sufficiently refined, even-odd clusters emerge, indicating that using masking schemes that are less algebraically compatible with practical leakage functions, like prime-field masking [11], could also be beneficial for protecting against DLSCA.

Profiled attacks against real-world targets are often significantly more complex than idealized evaluation settings, where the same device is used for both profiling and attack. Differences between devices often result in worse performance when models trained on a profiling device are applied to the target [3]. In security evaluations, the same device is commonly used for both profiling and attack to represent the worst-case scenario where the device differences are minimal. As such, the attack sets of the considered targets are from the same device as the profiling set, which raises questions about the practical relevance of these results for real-world settings. However, this work considers post-hoc explanations for models that already break a target. Therefore, the experimental evaluations emulate what is possible even for (more realistic) non-profiled adversaries that obtain a trained model using techniques like [45], as non-profiled attacks always consider a single device.

Doing similar analyses in practice might still be difficult, especially for side-channel evaluators with limited expertise in DL. This work is then aimed at highlighting that ambitious post-hoc interpretability in DLSCA is feasible. Future work can build on these results to find more automated approaches to aid evaluators in performing these analyses in practice. Notably, automatically finding relevant features by matching novel model outputs to (variations of) features found in this work using, e.g., KL-Divergence, seems promising. Variations here can include what leakage model is expected (e.g., which bits leak, using Hamming Distance between operations over HW) and what specific operations leak (e.g., using earlier/later operations in AES).

7 Conclusions and Future Work

We show that interpreting neural networks trained on side-channel models is feasible, even without access to random masks. Moreover, we highlight the effectiveness of investigating the structures learned during discrete steps in model performance and find evidence for the weak universality of circuits in side-channel models. Finally, we leverage these insights to reverse engineer the mask values. Automating these analyses represents an interesting direction for future work. Additionally, further work on leveraging the insights into DLSCA models to improve evaluation methods could be useful. For example, using tailored leakage models that consider common structures could help simplify model tuning. Finally, we only focus on MLPs (and a CNN in Appendix G) as these networks provide state-of-the-art attack performance for the tested targets. Extending this to Transformer-based architectures also used in DLSCA [16, 15] is an interesting direction for future work.

Acknowledgments

The authors would like to thank Gorka Abad, Abraham Basurto-Becerra, Azade Rezaeezade and anonymous reviewers for valuable feedback which helped improve this work. This work was (in part) supported by the Dutch Research Council (NWO) through the Challenges in Cyber Security (CiCS) project of the Gravitation research program under the grant 024.006.037, and through the PROACT project with grant number NWA.1215.18.014.

References

[1] Guillaume Alain and Yoshua Bengio. "Understanding intermediate layers using linear classifier probes". In: *5th International Conference on Learning Representations, ICLR 2017, Toulon, France, April 24-26, 2017, Workshop Track Proceedings*. OpenReview.net, 2017. URL: https://openreview.net/forum?id=HJ4-rAVtl.

[2] Ryad Benadjila et al. "Deep learning for side-channel analysis and introduction to ASCAD database". In: *J. Cryptogr. Eng.* 10.2 (2020), pp. 163–188. DOI: 10.1007/S13389-019-00220-8. URL: https://doi.org/10.1007/s13389-019-00220-8.

[3] Shivam Bhasin et al. “Mind the Portability: A Warriors Guide through Realistic Profiled Side-channel Analysis”. In: (2020). URL: https://www.ndss-symposium.org/ndss-paper/mind-the-portability-a-warriors-guide-through-realistic-profiled-side-channel-analysis/.

[4] Trenton Bricken et al. “Towards Monosemanticity: Decomposing Language Models With Dictionary Learning”. In: *Transformer Circuits Thread* (2023). URL: https://transformer-circuits.pub/2023/monosemantic-features/index.html.

[5] Olivier Bronchain and François-Xavier Standaert. “Breaking Masked Implementations with Many Shares on 32-bit Software Platforms or When the Security Order Does Not Matter”. In: *IACR Trans. Cryptogr. Hardw. Embed. Syst.* 2021.3 (2021), pp. 202–234. DOI: 10.46586/TCHES.V2021.I3.202-234. URL: https://doi.org/10.46586/tches.v2021.i3.202-234.

[6] Suresh Chari, Josyula R. Rao, and Pankaj Rohatgi. “Template Attacks”. In: *Cryptographic Hardware and Embedded Systems - CHES 2002, 4th International Workshop, Redwood Shores, CA, USA, August 13-15, 2002, Revised Papers*. Ed. by Burton S. Kaliski Jr., Çetin Kaya Koç, and Christof Paar. Vol. 2523. Lecture Notes in Computer Science. Springer, 2002, pp. 13–28. DOI: 10.1007/3-540-36400-5_3. URL: https://doi.org/10.1007/3-540-36400-5_3.

[7] Bilal Chughtai, Lawrence Chan, and Neel Nanda. “A Toy Model of Universality: Reverse Engineering how Networks Learn Group Operations”. In: *International Conference on Machine Learning, ICML 2023, 23-29 July 2023, Honolulu, Hawaii, USA*. Ed. by Andreas Krause et al. Vol. 202. Proceedings of Machine Learning Research. PMLR, 2023, pp. 6243–6267. URL: https://proceedings.mlr.press/v202/chughtai23a.html.

[8] Arthur Conmy et al. “Towards Automated Circuit Discovery for Mechanistic Interpretability”. In: *Advances in Neural Information Processing Systems*. Ed. by A. Oh et al. Vol. 36. Curran Associates, Inc., 2023, pp. 16318–16352. URL: https://proceedings.neurips.cc/paper_files/paper/2023/file/34e1dbe95d34d7ebaf99b9bcaeb5b2be-Paper-Conference.pdf.

[9] Joan Daemen and Vincent Rijmen. *The Design of Rijndael: AES - The Advanced Encryption Standard*. Information Security and Cryptography. Springer, 2002. ISBN: 3-540-42580-2. DOI: 10.1007/978-3-662-04722-4. URL: https://doi.org/10.1007/978-3-662-04722-4.

[10] Nelson Elhage et al. “Toy Models of Superposition”. In: *Transformer Circuits Thread* (2022). URL: https://transformer-circuits.pub/2022/toy_model/index.html.

[11] Sebastian Faust et al. “Connecting Leakage-Resilient Secret Sharing to Practice: Scaling Trends and Physical Dependencies of Prime Field Masking”. In: *Advances in Cryptology - EUROCRYPT 2024 - 43rd Annual International Conference on the Theory and Applications of Cryptographic Techniques, Zurich, Switzerland, May 26-30, 2024, Proceedings, Part IV*. Ed. by Marc Joye and Gregor Leander. Vol. 14654. Lecture Notes in Computer Science. Springer, 2024, pp. 316–344. DOI: 10.1007/978-3-031-58737-5_12. URL: https://doi.org/10.1007/978-3-031-58737-5_12.

[12] Federal Office for Information Security (BSI). *Guidelines for Evaluating Machine-Learning based Side-Channel Attack Resistance*. https://www.bsi.bund.de/SharedDocs/Downloads/DE/BSI/Zertifizierung/Interpretationen/AIS_46_AI_guide.pdf?__blob=publicationFile&v=6. Technical Report AIS 46. Feb. 2024.

[13] Si Gao et al. “Non-profiled Mask Recovery: The Impact of Independent Component Analysis”. In: *Smart Card Research and Advanced Applications, 17th International Conference, CARDIS 2018, Montpellier, France, November 12-14, 2018, Revised Selected Papers*. Ed. by Begül Bilgin and Jean-Bernard Fischer. Vol. 11389. Lecture Notes in Computer Science. Springer, 2018, pp. 51–64. DOI: 10.1007/978-3-030-15462-2_4. URL: https://doi.org/10.1007/978-3-030-15462-2_4.

[14] Atticus Geiger et al. “Causal Abstractions of Neural Networks”. In: *Advances in Neural Information Processing Systems 34: Annual Conference on Neural Information Processing Systems 2021, NeurIPS 2021, December 6-14, 2021, virtual*. Ed. by Marc'Aurelio Ranzato et al. 2021, pp. 9574–9586. URL: https://proceedings.neurips.cc/paper/2021/hash/4f5c422f4d49a5a807eda27434231040-Abstract.html.

[15] Suvadeep Hajra, Siddhartha Chowdhury, and Debdeep Mukhopadhyay. "EstraNet: An Efficient Shift-Invariant Transformer Network for Side-Channel Analysis". In: *IACR Trans. Cryptogr. Hardw. Embed. Syst.* 2024.1 (2024), pp. 336–374. DOI: 10.46586/TCHES.V2024.I1.336-374. URL: https://doi.org/10.46586/tches.v2024.i1.336-374.

[16] Suvadeep Hajra et al. "TransNet: Shift Invariant Transformer Network for Side Channel Analysis". In: *Progress in Cryptology - AFRICACRYPT 2022: 13th International Conference on Cryptology in Africa, AFRICACRYPT 2022, Fes, Morocco, July 18-20, 2022, Proceedings*. Ed. by Lejla Batina and Joan Daemen. Vol. 13503. Lecture Notes in Computer Science. Springer Nature Switzerland, 2022, pp. 371–396. DOI: 10.1007/978-3-031-17433-9_16. URL: https://doi.org/10.1007/978-3-031-17433-9_16.

[17] Stefan Heimersheim and Neel Nanda. "How to use and interpret activation patching". In: *CoRR* abs/2404.15255 (2024). DOI: 10.48550/ARXIV.2404.15255. arXiv: 2404.15255. URL: https://doi.org/10.48550/arXiv.2404.15255.

[18] Benjamin Hettwer, Stefan Gehrer, and Tim Güneysu. "Deep Neural Network Attribution Methods for Leakage Analysis and Symmetric Key Recovery". In: *Selected Areas in Cryptography - SAC 2019 - 26th International Conference, Waterloo, ON, Canada, August 12-16, 2019, Revised Selected Papers*. Ed. by Kenneth G. Paterson and Douglas Stebila. Vol. 11959. Lecture Notes in Computer Science. Springer, 2019, pp. 645–666. DOI: 10.1007/978-3-030-38471-5_26. URL: https://doi.org/10.1007/978-3-030-38471-5_26.

[19] Yongbo Hu et al. "Machine learning and side channel analysis in a CTF competition". In: *IACR Cryptol. ePrint Arch.* (2019), p. 860. URL: https://eprint.iacr.org/2019/860.

[20] Yuval Ishai, Amit Sahai, and David A. Wagner. "Private Circuits: Securing Hardware against Probing Attacks". In: *Advances in Cryptology - CRYPTO 2003, 23rd Annual International Cryptology Conference, Santa Barbara, California, USA, August 17-21, 2003, Proceedings*. Ed. by Dan Boneh. Vol. 2729. Lecture Notes in Computer Science. Springer, 2003, pp. 463–481. DOI: 10.1007/978-3-540-45146-4_27. URL: https://doi.org/10.1007/978-3-540-45146-4_27.

[21] Akira Ito, Rei Ueno, and Naofumi Homma. "On the Success Rate of Side-Channel Attacks on Masked Implementations: Information-Theoretical Bounds and Their Practical Usage". In: *Proceedings of the 2022 ACM SIGSAC Conference on Computer and Communications Security, CCS 2022, Los Angeles, CA, USA, November 7-11, 2022*. Ed. by Heng Yin et al. ACM, 2022, pp. 1521–1535. DOI: 10.1145/3548606.3560579. URL: https://doi.org/10.1145/3548606.3560579.

[22] Sengim Karayalcin, Marina Krcek, and Stjepan Picek. *A Practical Tutorial on Deep Learning-based Side-channel Analysis*. Cryptology ePrint Archive, Paper 2025/471. 2025. URL: https://eprint.iacr.org/2025/471.

[23] Paul C. Kocher, Joshua Jaffe, and Benjamin Jun. "Differential Power Analysis". In: *Advances in Cryptology - CRYPTO '99, 19th Annual International Cryptology Conference, Santa Barbara, California, USA, August 15-19, 1999, Proceedings*. Ed. by Michael J. Wiener. Vol. 1666. Lecture Notes in Computer Science. Springer, 1999, pp. 388–397. DOI: 10.1007/3-540-48405-1_25. URL: https://doi.org/10.1007/3-540-48405-1_25.

[24] Kenneth Li et al. "Emergent World Representations: Exploring a Sequence Model Trained on a Synthetic Task". In: *The Eleventh International Conference on Learning Representations, ICLR 2023, Kigali, Rwanda, May 1-5, 2023*. OpenReview.net, 2023. URL: https://openreview.net/forum?id=DeG07_TcZvT.

[25] Houssem Maghrebi, Thibault Portigliatti, and Emmanuel Prouff. "Breaking Cryptographic Implementations Using Deep Learning Techniques". In: *Security, Privacy, and Applied Cryptography Engineering - 6th International Conference, SPACE 2016, Hyderabad, India, December 14-18, 2016, Proceedings*. Ed. by Claude Carlet, M. Anwar Hasan, and Vishal Saraswat. Vol. 10076. Lecture Notes in Computer Science. Springer, 2016, pp. 3–26. DOI: 10.1007/978-3-319-49445-6_1. URL: https://doi.org/10.1007/978-3-319-49445-6__1.

[26] Loïc Masure, Cécile Dumas, and Emmanuel Prouff. "Gradient Visualization for General Characterization in Profiling Attacks". In: *Constructive Side-Channel Analysis and Secure Design - 10th International Workshop, COSADE 2019, Darmstadt, Germany, April 3-5, 2019, Proceedings*. Ed. by Ilia Polian and Marc Stöttinger. Vol. 11421. Lecture Notes in Computer Science. Springer, 2019, pp. 145–167. DOI: 10.1007/978-3-030-16350-1_9. URL: https://doi.org/10.1007/978-3-030-16350-1_9.

[27] Loïc Masure et al. “Don’t Learn What You Already Know Scheme-Aware Modeling for Profiling Side-Channel Analysis against Masking”. In: *IACR Trans. Cryptogr. Hardw. Embed. Syst.* 2023.1 (2023), pp. 32–59. DOI: 10.46586/TCHES.V2023.I1.32-59. URL: https://doi.org/10.46586/tches.v2023.i1.32-59.

[28] Eric J. Michaud et al. “The Quantization Model of Neural Scaling”. In: *Advances in Neural Information Processing Systems 36: Annual Conference on Neural Information Processing Systems 2023, NeurIPS 2023, New Orleans, LA, USA, December 10 - 16, 2023*. Ed. by Alice Oh et al. 2023. URL: http://papers.nips.cc/paper_files/paper/2023/hash/5b6346a05a537d4cdb2f50323452a9fe-Abstract-Conference.html.

[29] Neel Nanda, Andrew Lee, and Martin Wattenberg. “Emergent Linear Representations in World Models of Self-Supervised Sequence Models”. In: *Proceedings of the 6th BlackboxNLP Workshop: Analyzing and Interpreting Neural Networks for NLP, BlackboxNLP@EMNLP 2023, Singapore, December 7, 2023*. Ed. by Yonatan Belinkov et al. Association for Computational Linguistics, 2023, pp. 16–30. DOI: 10.18653/V1/2023.BLACKBOXNLP-1.2. URL: https://doi.org/10.18653/v1/2023.blackboxnlp-1.2.

[30] Neel Nanda et al. “Progress measures for grokking via mechanistic interpretability”. In: *The Eleventh International Conference on Learning Representations, ICLR 2023, Kigali, Rwanda, May 1-5, 2023*. OpenReview.net, 2023. URL: https://openreview.net/forum?id=9XFSbDPmdW.

[31] Chris Olah. *Mechanistic Interpretability, Variables, and the Importance of Interpretable Bases*. June 27, 2022. URL: https://www.transformer-circuits.pub/2022/mech-interp-essay (visited on 01/21/2025).

[32] Chris Olah et al. “Zoom in: An introduction to circuits”. In: *Distill* 5.3 (2020), e00024–001.

[33] Catherine Olsson et al. “In-context Learning and Induction Heads”. In: *Transformer Circuits Thread* (2022). URL: https://transformer-circuits.pub/2022/in-context-learning-and-induction-heads/index.html.

[34] Guilherme Perin, Lichao Wu, and Stjepan Picek. “Exploring Feature Selection Scenarios for Deep Learning-based Side-channel Analysis”. In: *IACR Trans. Cryptogr. Hardw. Embed. Syst.* 2022.4 (2022), pp. 828–861. DOI: 10.46586/TCHES.V2022.I4.828-861. URL: https://doi.org/10.46586/tches.v2022.i4.828-861.

[35] Guilherme Perin et al. *I Know What Your Layers Did: Layer-wise Explainability of Deep Learning Side-channel Analysis*. Cryptology ePrint Archive, Paper 2022/1087. 2022. URL: https://eprint.iacr.org/2022/1087.

[36] Stjepan Picek et al. “SoK: Deep Learning-based Physical Side-channel Analysis”. In: *ACM Comput. Surv.* 55.11 (2023), 227:1–227:35. DOI: 10.1145/3569577. URL: https://doi.org/10.1145/3569577.

[37] Alethea Power et al. “Grokking: Generalization Beyond Overfitting on Small Algorithmic Datasets”. In: *CoRR* abs/2201.02177 (2022). arXiv: 2201.02177. URL: https://arxiv.org/abs/2201.02177.

[38] Mathieu Renauld et al. “A Formal Study of Power Variability Issues and Side-Channel Attacks for Nanoscale Devices”. In: *Advances in Cryptology - EUROCRYPT 2011 - 30th Annual International Conference on the Theory and Applications of Cryptographic Techniques, Tallinn, Estonia, May 15-19, 2011. Proceedings*. Ed. by Kenneth G. Paterson. Vol. 6632. Lecture Notes in Computer Science. Springer, 2011, pp. 109–128. DOI: 10.1007/978-3-642-20465-4_8. URL: https://doi.org/10.1007/978-3-642-20465-4_8.

[39] Jorai Rijsdijk, Lichao Wu, and Guilherme Perin. “Reinforcement Learning-Based Design of Side-Channel Countermeasures”. In: *Security, Privacy, and Applied Cryptography Engineering - 11th International Conference, SPACE 2021, Kolkata, India, December 10-13, 2021, Proceedings*. Ed. by Lejla Batina, Stjepan Picek, and Mainack Mondal. Vol. 13162. Lecture Notes in Computer Science. Springer, 2021, pp. 168–187. DOI: 10.1007/978-3-030-95085-9_9. URL: https://doi.org/10.1007/978-3-030-95085-9_9.

[40] Thomas Roche. *EUCLEAK Side-Channel Attack on the YubiKey 5 Series (Revealing and Breaking Infineon ECDSA Implementation on the Way)*. 2024. URL: https://ninjalab.io/wp-content/uploads/2024/10/20241022_eucleak.pdf.

[41] Thomas Roche et al. “A Side Journey To Titan”. In: *30th USENIX Security Symposium (USENIX Security 21)*. USENIX Association, Aug. 2021, pp. 231–248. ISBN: 978-1-939133-24-3. URL: https://www.usenix.org/conference/usenixsecurity21/presentation/roche.

[42] James B. Simon et al. “On the Stepwise Nature of Self-Supervised Learning”. In: *International Conference on Machine Learning, ICML 2023, 23-29 July 2023, Honolulu, Hawaii, USA*. Ed. by Andreas Krause et al. Vol. 202. Proceedings of Machine Learning Research. PMLR, 2023, pp. 31852–31876. URL: https://proceedings.mlr.press/v202/simon23a.html.

[43] François-Xavier Standaert. *Side-Channel Analysis and Leakage-Resistance*. Version 1.2, 2024.

[44] François-Xavier Standaert, Tal Malkin, and Moti Yung. “A Unified Framework for the Analysis of Side-Channel Key Recovery Attacks”. In: *Advances in Cryptology - EUROCRYPT 2009, 28th Annual International Conference on the Theory and Applications of Cryptographic Techniques, Cologne, Germany, April 26-30, 2009. Proceedings*. Ed. by Antoine Joux. Vol. 5479. Lecture Notes in Computer Science. Springer, 2009, pp. 443–461. DOI: 10.1007/978-3-642-01001-9_26. URL: https://doi.org/10.1007/978-3-642-01001-9_26.

[45] Benjamin Timon. “Non-Profiled Deep Learning-based Side-Channel attacks with Sensitivity Analysis”. In: *IACR Trans. Cryptogr. Hardw. Embed. Syst.* 2019.2 (2019), pp. 107–131. DOI: 10.13154/TCHES.V2019.I2.107-131. URL: https://doi.org/10.13154/tches.v2019.i2.107-131.

[46] Daan van der Valk, Stjepan Picek, and Shivam Bhasin. “Kilroy Was Here: The First Step Towards Explainability of Neural Networks in Profiled Side-Channel Analysis”. In: *Constructive Side-Channel Analysis and Secure Design - 11th International Workshop, COSADE 2020, Lugano, Switzerland, April 1-3, 2020, Revised Selected Papers*. Ed. by Guido Marco Bertoni and Francesco Regazzoni. Vol. 12244. Lecture Notes in Computer Science. Springer, 2020, pp. 175–199. DOI: 10.1007/978-3-030-68773-1_9. URL: https://doi.org/10.1007/978-3-030-68773-1_9.

[47] Aurélien Vasselle, Hugues Thiebeauld, and Philippe Maurine. “Spatial dependency analysis to extract information from side-channel mixtures: extended version”. In: *J. Cryptogr. Eng.* 13.4 (2023), pp. 409–425. DOI: 10.1007/S13389-022-00307-9. URL: https://doi.org/10.1007/s13389-022-00307-9.

[48] Kevin Ro Wang et al. “Interpretability in the Wild: a Circuit for Indirect Object Identification in GPT-2 Small”. In: *The Eleventh International Conference on Learning Representations, ICLR 2023, Kigali, Rwanda, May 1-5, 2023*. OpenReview.net, 2023. URL: https://openreview.net/forum?id=NpsVSN6o4ul.

[49] Lichao Wu et al. “Ablation Analysis for Multi-Device Deep Learning-Based Physical Side-Channel Analysis”. In: *IEEE Trans. Dependable Secur. Comput.* 21.3 (2024), pp. 1331–1341. DOI: 10.1109/TDSC.2023.3278857. URL: https://doi.org/10.1109/TDSC.2023.3278857.

[50] Lichao Wu et al. “Label Correlation in Deep Learning-Based Side-Channel Analysis”. In: *IEEE Trans. Inf. Forensics Secur.* 18 (2023), pp. 3849–3861. DOI: 10.1109/TIFS.2023.3287728. URL: https://doi.org/10.1109/TIFS.2023.3287728.

[51] Trevor Yap, Stjepan Picek, and Shivam Bhasin. “OccPoIs: Points of Interest Based on Neural Network’s Key Recovery in Side-Channel Analysis Through Occlusion”. In: *Progress in Cryptology - INDOCRYPT 2024 - 25th International Conference on Cryptology in India, Chennai, India, December 18-21, 2024, Proceedings, Part II*. Ed. by Sourav Mukhopadhyay and Pantelimon Stanica. Vol. 15496. Lecture Notes in Computer Science. Springer, 2024, pp. 3–28. DOI: 10.1007/978-3-031-80311-6_1. URL: https://doi.org/10.1007/978-3-031-80311-6_1.

[52] Trevor Yap et al. “Peek into the Black-Box: Interpretable Neural Network using SAT Equations in Side-Channel Analysis”. In: *IACR Trans. Cryptogr. Hardw. Embed. Syst.* 2023.2 (2023), pp. 24–53. DOI: 10.46586/TCHES.V2023.I2.24-53. URL: https://doi.org/10.46586/tches.v2023.i2.24-53.

[53] Kota Yoshida, Sengim Karayalcin, and Stjepan Picek. “Can KANs Do It? Toward Interpretable Deep Learning-based Side-channel Analysis”. In: *IACR Cryptol. ePrint Arch.* (2024), p. 1570. URL: https://eprint.iacr.org/2024/1570.

[54] Gabriel Zaid et al. “Conditional Variational AutoEncoder based on Stochastic Attacks”. In: *IACR Trans. Cryptogr. Hardw. Embed. Syst.* 2023.2 (2023), pp. 310–357. DOI: 10.46586/TCHES.V2023.I2.310-357. URL: https://doi.org/10.46586/tches.v2023.i2.310-357.

[55] Gabriel Zaid et al. “Methodology for Efficient CNN Architectures in Profiling Attacks”. In: *IACR Transactions on Cryptographic Hardware and Embedded Systems* 2020.1 (Nov. 2019), pp. 1–36. DOI: 10.13154/tches.v2020.i1.1-36. URL: https://tches.iacr.org/index.php/TCHES/article/view/8391.

[56] Ziqian Zhong et al. “The Clock and the Pizza: Two Stories in Mechanistic Explanation of Neural Networks”. In: *Advances in Neural Information Processing Systems 36: Annual Conference on Neural Information Processing Systems 2023, NeurIPS 2023, New Orleans, LA, USA, December 10 - 16, 2023*. Ed. by Alice Oh et al. 2023. URL: http://papers.nips.cc/paper_files/paper/2023/hash/56cbfbf49937a0873d451343ddc8c57d-Abstract-Conference.html.

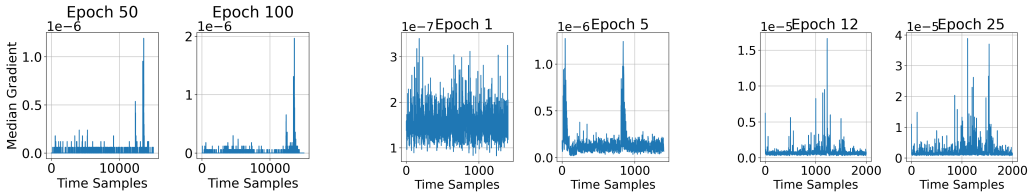

(a) CHES CTF (b) ESHARD (c) ASCADr

Figure 8: Gradient Visualization Example of MLP models on three datasets.

A Extended Related Work

The first main direction for interpreting what leakage neural networks exploit was the input visualization approach. Here, input attribution techniques from the vision domain were adopted to show regions of the traces that influence network predictions [18]. Several input attribution methods have been investigated, where examples include gradient-based visualizations in [26], weight-based visualizations in [55], and occlusion-based approaches [51]. In Figure 8 we show an example of gradient-based visualization for the MLPs used in this work. As we can see, the visualizations do highlight similar regions as we found using the secret-shares we extracted. However, from only these plots it is difficult to extract meaningful insights without access to secret-share randomness. In the works proposing these explainability approaches, visualization is often compared with ground-truth leakage information using SNR for known secret-shares (as we do using extracted shares), which can then highlight the leakage from which shares the network is exploiting [26, 18]. However, this assumes knowledge of masking randomness.

More recently, the internals of networks have also been analyzed. Van der Valk et al. [46] compared networks trained on different side-channel datasets, showing that these networks are often very different from each other. Wu et al. [49] used ablations to evaluate the roles of specific layers in defeating certain countermeasures. In Perin et al. [35], the probes are trained at each layer for several (ir)relevant secret shares, showing that an information bottleneck forms, resulting in the compression of irrelevant share information while relevant values are maintained.

Finally, there are two works that propose using more interpretable architectures for DLSCA. Yap et al. used a truth table convolutional network to find SAT-equations for important points in the trace [52]. Yoshida et al. used Kolmogorov-Arnold networks [53]. These works show nice interpretations of network behavior, but these interpretations are only shown on simulations or selected informative features. The interpretability benefits of using these architectures trained on full-length traces are still an open question, as the additional (non-informative) points result in less 'clean' interpretations. These more interpretable architectures also come at an additional computational cost, while resulting in worse attacks, limiting their relevance as practical replacements for standard MLPs and CNNs.

Overall, these works provide limited insights into how certain countermeasures are defeated. Although some approaches can show which shares are (not) exploited, these require access to masking randomness during training, which is not always possible. Our work provides an approach that allows us to interpret standard neural network architectures, while minimizing the necessary assumptions beyond a network that can break a target. Besides this, our approach is the only approach that allows for the extraction of secret shares.

B Datasets

We utilize publicly available datasets commonly used in SCA literature for benchmarking. These datasets implement AES-128 with Boolean masking protection. The attack set consists of 10 000 traces for each dataset.

CHES CTF 2018 [19][11] consists of power consumption measurements from an AES-128 implementation running on ARM Cortex-M4 (32 bits). CHES CTF 2018 raw traces contain 650 000 sample

[11] Referred to as CHES_CTF.

points per trace. Following [34], we take a subset of 150 000 points corresponding to the initial setup and the first AES round and resample to 15 000 samples per trace. The profiling set has 30 000 traces.

ESHARD-AES128 [47][12] consists of EM measurements from a software-masked AES-128 implementation running on an ARM Cortex-M4 device. The AES implementation is protected with a first-order Boolean masking scheme and shuffling of the `S-box` operations. In this work, we consider a trimmed version of the dataset that is publicly available [13] and includes the processing of the masks and all `S-box` operations in the first encryption round without shuffling. This dataset contains 100 000 measurements with 90 000 traces for the profiling set.

ASCAD [2] measures EM emissions from an AES-128 implementation on AVR RISC (8 bits). We use the version with the variable key in the profiling set. The traces are 250 000 sample points per trace. Following [35], we take a window of 20 000 points, which are resampled to 2 000 points. 200 000 traces are used for profiling.

C Models and Training

The used models are MLPs from [35], where model configurations were found through a random hyperparameter search for ESHARD and ASCAD. Note that, as the ESHARD model performed well directly for CHES_CTF, we did not do further optimizations.

The model for CHES_CTF and ESHARD is a 4-layer MLP with 40 neurons in each layer with *he_uniform* weight initialization. We use *relu* activations. We use the Adam optimizer with a learning rate of 0.0025 and L1 regularization set to 0.000075. The batch size is 400, and we train for 200 epochs for CHES_CTF and 100 for ESHARD.

For ASCAD, the model is a 6-layer MLP with 100 neurons in each layer with *random_uniform* weight initialization. We use the Adam optimizer with a learning rate of 0.0005. We use *elu* activations, and we again train for 100 epochs with a batch size of 400.

D Computational Load

Training these models takes under an hour on a desktop workstation with 64GB RAM and an NVIDIA 4080 GPU. Producing PI/probe plots per epoch takes a similar time (mainly because of reloading models for every epoch from disk). All other experiments take negligible compute (seconds, sometimes minutes).

E ESHARD Results

In Figure 9, we see that for ESHARD, only one phase transition occurs for the test set. At epoch 4, the perceived information becomes positive, and the models start to generalize. We note that the main distinction here is again the high-low HWs, similar to the first step in CHES_CTF. Further analyses are analogous to CHES_CTF, although the model here can never distinguish between even and odd HWs.

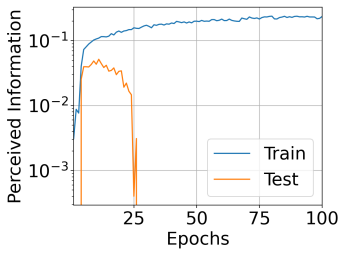

Figure 9: Evolution of Perceived Information for train and test traces of the ESHARD dataset.

[12] Referred to as ESHARD.

[13] `https://gitlab.com/eshard/nucleo_sw_aes_masked_shuffled`

In the two rightmost plots in Figure 10, we showcase distributions of the concrete intermediate values the models use. The models are clearly mapping the HWs of secret shares onto specific features.

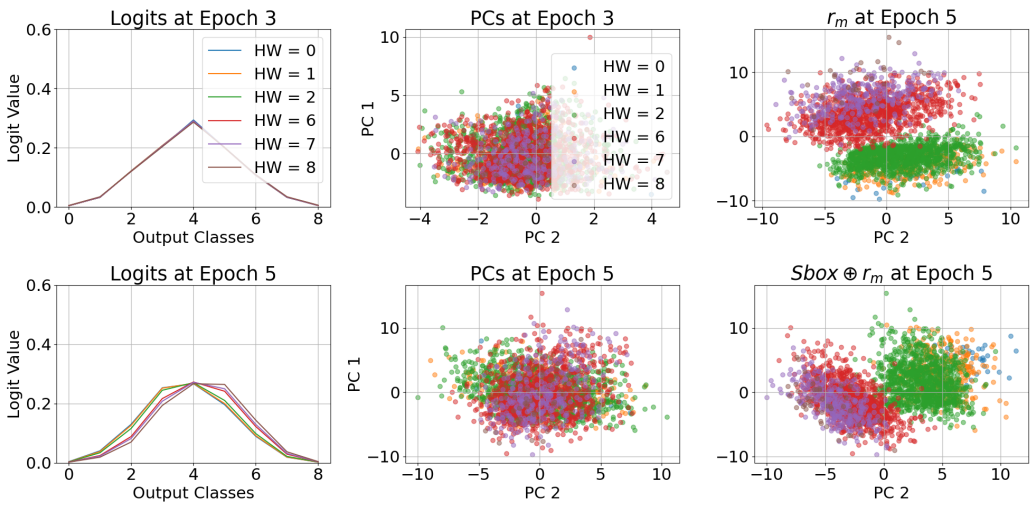

Figure 10: Logit analysis (first column) and activation analysis (second column) from models at epoch 3 (top row) and epoch 5 (bottom row). The legend is shared among all figures. We also include the PC embeddings for the actual mask of secret shares at epoch 5 (third column). The masks we extract are in Figure 11.

E.1 Activation Patching

We can do similar patching experiments as done for CHES_CTF in Section 4.1. As the high-low HWs are not on the diagonals in the PCs at epoch 5, we rotate the PC coordinates before patching and then rotate them back before continuing inference to align PCs more with the expected masks. The results we see in Figure 11 closely match the actual distributions of secret share HWs as seen in the rightmost plots of Figure 10.

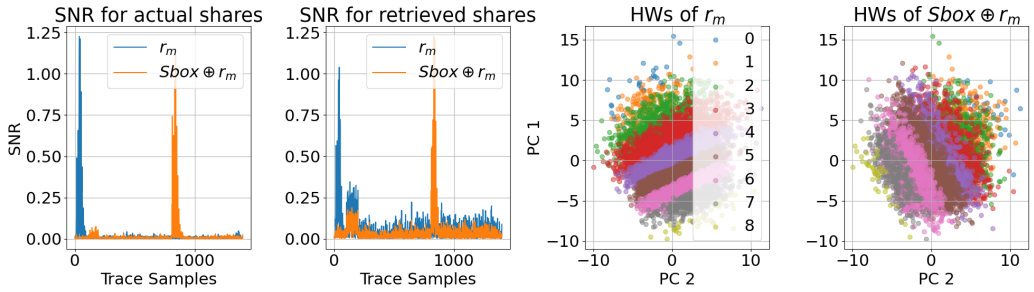

Figure 11: SNR plot and PC component distributions for mask values using patching experiments in ESHARD.

F ASCAD Patching results

As the leakage model for ASCAD is more complicated than the HW models, patching becomes more difficult. First, we train probes on the final layer to classify the input and output bits separately. We can directly measure the effects on only the input or the output. Patching the input shares in the PC components in layer 2, which we show in Figure 7, does not work. Then, we find a qualitatively similar structure in PC1 and PC2 in layer one and patch there.

For the patches on the output shares, we set the first two components, which are related to the input shares, to 0 to isolate the effects of the patched components. For both experiments, we again rotate the two components by multiplying them with a rotation matrix to simplify the patches.

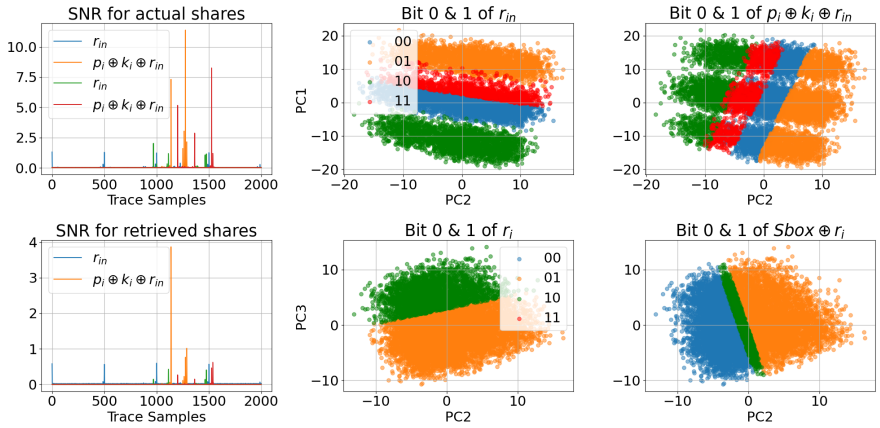

Figure 12: SNR plot and PC component distributions for mask values using patching experiments in ASCAD.

In Figure 12, we can see that the patches work reasonably well. Clearly, intervening on the found components has some causal effects. Furthermore, as we can see in the SNR plots, the patched outputs of the models are tied to the mask values we expect. However, the SNR values are significantly lower than those for the actual shares, and the r_i and $\texttt{S-box} \oplus r_i$ shares only result in two or three classes, respectively, where we expect four. Additionally, the reversed shares do not combine to the correct label for the input bits, indicating that while the mask values we retrieve are a reasonable clustering, further post-processing is necessary to retrieve the actual values.

As we aim to keep the experiments (somewhat) aligned across all targets, we do not tailor the patching methods further for ASCAD. The current experiments show we can intervene in the structures and observe effects on the (probe) outputs. However, refining mask extraction methods in models with more complicated interactions is an interesting direction for future work. We provide further analysis to validate model predictions based on the four bits in Appendix I.1.

G ASCAD CNN

To see whether analyses are feasible for CNNs, we consider the CNN used for the ASCAD target from [35]. In Figure 13, we see that the bits that show significantly increased accuracies are the same

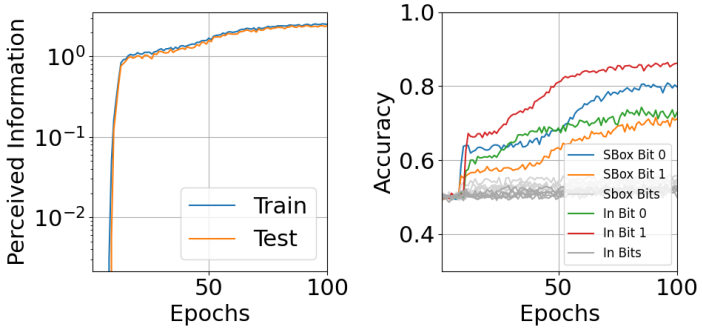

Figure 13: Evolution of Perceived Information and probe accuracies for bits during training for the ASCAD dataset for CNN.

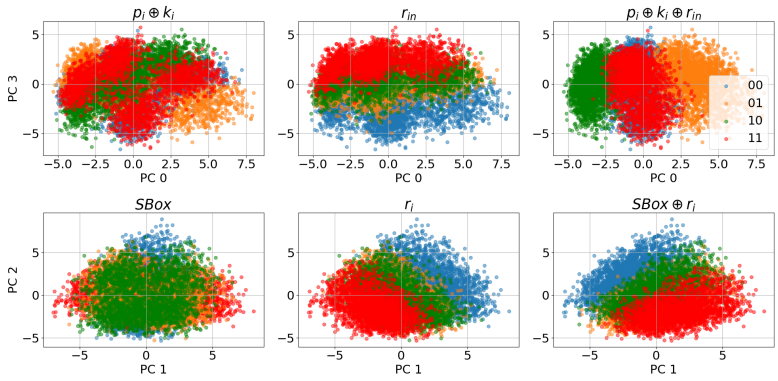

Figure 14: PC structures for ASCAD CNN after the third convolutional block.

as in Figure 6. However, the performance increase (after initial, smaller jumps) is more gradual. This, and the model having significantly more layers to check, results in it being somewhat more difficult to find the structures.

As the performance increases steadily, we focus our analysis on the final model at epoch 100 and show these in Figure 14. We note that in this case, shares are still in the first 4 PCs, but the input shares are not the first 2 PCs, but PC 0 and 2 (output shares PC 1 and 3).

H HW Recombination CHES_CTF and ESHARD

Next, we discuss how mask recombination can be done algorithmically for the HW leakage model.

H.1 High-Low HW Distinguishing

For the CHES_CTF and ESHARD targets, we notice that after the first performance increase (for some cases), high and low HWs can be differentiated. These are byte-based implementations protected with Boolean masking with order 2, i.e., the sensitive value $x = x_1 \oplus x_2$ ($\oplus$ being bitwise xor). When, based on prior experience working with these targets, we then choose to model the leakage (and therefore the presumed features of the model) as the $L = HW(x_i)$[14] we can consider modeling how occurrences of different classes $Y = HW(x)$ look. In Table 1, low HWs tend to be on the diagonal from top-left to bottom-right, while high HWs tend to be on the other diagonal. This (low HWs on one diagonal while high HWs are on the other) matches the PC embeddings for both models in Figure 10 and Figure 3.

H.2 Even-Odd HW Distinguishing CHES_CTF

For CHES_CTF, we further see that the even and odd HW target classes can be distinguished after the second performance jump. From Table 1, it is clear that if the HWs of each secret share can be retrieved accurately enough, there should be a clear separation between even and odd HWs for the resulting point. Indeed, for any point $HW(x_1), HW(x_2)$ where $x = x_1 \oplus x_2$ we have that $HW(x_1) + HW(x_2) \bmod 2 = HW(x) \bmod 2$. This can be seen in Table 1 for two 8-bit shares, but the ability to distinguish the parity of $HW(x)$ holds for general higher masking orders d [21].

I Bitwise Leakage ASCAD

As we show in Figure 6, the features the model learns for ASCAD are the two least significant bits of both $p_i \oplus k_i$ and $\texttt{S-box}[p_i \oplus k_i]$. We first note that the way the first two bits of $\texttt{S-box}[p_i \oplus k_i]$ relate to model labels ($\texttt{S-box}[p_i \oplus k_i]$) is straightforward: if bits 0 and 1 of $\texttt{S-box}[p_i \oplus k_i]$ are 00,

[14] We note that we knew this a priori for ESHARD and it was strongly suspected for CHES_CTF. However, it is also a common leakage model in practice.

$HW(x)$	Matrices counting occurrences of $HW(s_1), HW(s_2)$ s.t. $x = s_1 \oplus s_2$ from 0-9.
HW = 0 HW = 1	$\begin{bmatrix} 1 & 8 & 0 & 0 & 0 & 0 & 0 & 0 & 0 \\ 8 & 8 & 56 & 0 & 0 & 0 & 0 & 0 & 0 \\ 0 & 56 & 28 & 168 & 0 & 0 & 0 & 0 & 0 \\ 0 & 0 & 168 & 56 & 280 & 0 & 0 & 0 & 0 \\ 0 & 0 & 0 & 280 & 70 & 280 & 0 & 0 & 0 \\ 0 & 0 & 0 & 0 & 280 & 56 & 168 & 0 & 0 \\ 0 & 0 & 0 & 0 & 0 & 168 & 28 & 56 & 0 \\ 0 & 0 & 0 & 0 & 0 & 0 & 56 & 8 & 8 \\ 0 & 0 & 0 & 0 & 0 & 0 & 0 & 8 & 1 \end{bmatrix}$
HW = 2 HW = 3	$\begin{bmatrix} 0 & 0 & 28 & 56 & 0 & 0 & 0 & 0 & 0 \\ 0 & 56 & 168 & 168 & 280 & 0 & 0 & 0 & 0 \\ 28 & 168 & 336 & 840 & 420 & 560 & 0 & 0 & 0 \\ 56 & 168 & 840 & 840 & 1680 & 560 & 560 & 0 & 0 \\ 0 & 280 & 420 & 1680 & 1120 & 1680 & 420 & 280 & 0 \\ 0 & 0 & 560 & 560 & 1680 & 840 & 840 & 168 & 56 \\ 0 & 0 & 0 & 560 & 420 & 840 & 336 & 168 & 28 \\ 0 & 0 & 0 & 0 & 280 & 168 & 168 & 56 & 0 \\ 0 & 0 & 0 & 0 & 0 & 56 & 28 & 0 & 0 \end{bmatrix}$
HW = 4	$\begin{bmatrix} 0 & 0 & 0 & 0 & 70 & 0 & 0 & 0 & 0 \\ 0 & 0 & 0 & 280 & 0 & 280 & 0 & 0 & 0 \\ 0 & 0 & 420 & 0 & 1120 & 0 & 420 & 0 & 0 \\ 0 & 280 & 0 & 1680 & 0 & 1680 & 0 & 280 & 0 \\ 70 & 0 & 1120 & 0 & 2520 & 0 & 1120 & 0 & 70 \\ 0 & 280 & 0 & 1680 & 0 & 1680 & 0 & 280 & 0 \\ 0 & 0 & 420 & 0 & 1120 & 0 & 420 & 0 & 0 \\ 0 & 0 & 0 & 280 & 0 & 280 & 0 & 0 & 0 \\ 0 & 0 & 0 & 0 & 70 & 0 & 0 & 0 & 0 \end{bmatrix}$
HW = 5 HW = 6	$\begin{bmatrix} 0 & 0 & 0 & 0 & 0 & 56 & 28 & 0 & 0 \\ 0 & 0 & 0 & 0 & 280 & 168 & 168 & 56 & 0 \\ 0 & 0 & 0 & 560 & 420 & 840 & 336 & 168 & 28 \\ 0 & 0 & 560 & 560 & 1680 & 840 & 840 & 168 & 56 \\ 0 & 280 & 420 & 1680 & 1120 & 1680 & 420 & 280 & 0 \\ 56 & 168 & 840 & 840 & 1680 & 560 & 560 & 0 & 0 \\ 28 & 168 & 336 & 840 & 420 & 560 & 0 & 0 & 0 \\ 0 & 56 & 168 & 168 & 280 & 0 & 0 & 0 & 0 \\ 0 & 0 & 28 & 56 & 0 & 0 & 0 & 0 & 0 \end{bmatrix}$
HW = 7 HW = 8	$\begin{bmatrix} 0 & 0 & 0 & 0 & 0 & 0 & 0 & 8 & 1 \\ 0 & 0 & 0 & 0 & 0 & 0 & 56 & 8 & 8 \\ 0 & 0 & 0 & 0 & 0 & 168 & 28 & 56 & 0 \\ 0 & 0 & 0 & 0 & 280 & 56 & 168 & 0 & 0 \\ 0 & 0 & 0 & 280 & 70 & 280 & 0 & 0 & 0 \\ 0 & 0 & 168 & 56 & 280 & 0 & 0 & 0 & 0 \\ 0 & 56 & 28 & 168 & 0 & 0 & 0 & 0 & 0 \\ 8 & 8 & 56 & 0 & 0 & 0 & 0 & 0 & 0 \\ 1 & 8 & 0 & 0 & 0 & 0 & 0 & 0 & 0 \end{bmatrix}$

Table 1: Occurrences of HWs for two 8-bit shares for each of the nine output classes, cell i, j in each matrix corresponds to $HW(s_1), HW(s_2)$. For the percentage of examples in practice, these values should be divided by 256^2. As even and odd $HW(x)$ never occur in the same place, we show two HWs in one matrix. Note that any red value (resp. black) is a zero in black (resp. red).

then these correspond to predicting each label $y \mod 4 \equiv 0$. For bits 0 and 1 of $p_i \oplus k_i$, we can use the inverse of the S-box[15]. If we define $y' = \text{S-Box}^{-1}[y]$ then if bit 0 and 1 of $p_i \oplus k_i$ are 00, we predict y s.t. $y' \mod 4 \equiv 0$.

Combining these, we can divide the output classes into 16 clusters corresponding to model predictions. Practically, we define the outputs that belong to the 16 classes as $Y_i = \{y | y \equiv i \mod 4 \wedge y' \equiv \lfloor \frac{i}{4} \rfloor \mod 4\}$. Here, we set i to be a concatenation of bit 1 and 0 of $p_i \oplus k_i$ and then bit 1 and 0 of S-box$[p_i \oplus k_i]$.

[15]The AES S-box is bijective, which simplifies this, but the analysis also works for surjective functions by taking the pre-image.

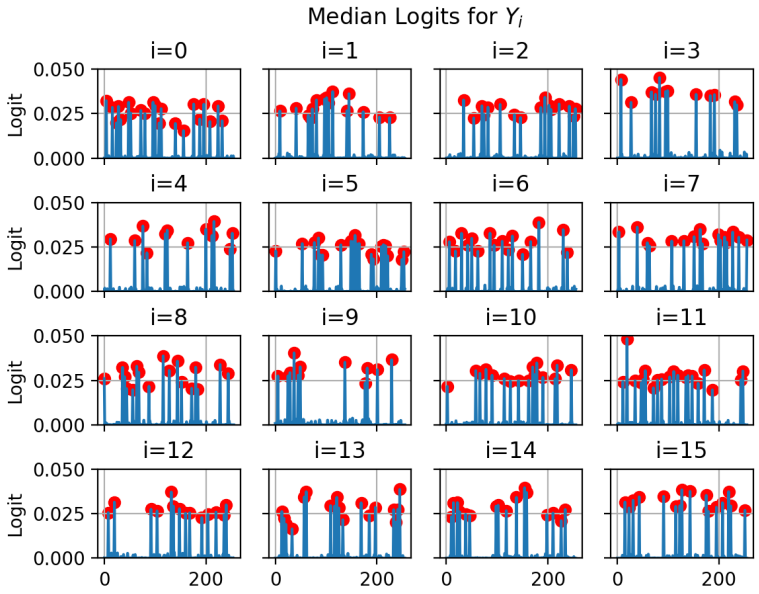

Figure 15: Median logits for traces belonging to varying Y_i classes. The red dots indicate indices in the respective Y_i.

We can then train a linear probe on the activations of the final layer to predict these 16 classes. If we then transform the probe outputs to evenly distribute the predictions for its i'th output to the values in Y_i, we can measure the entropy between this resulting distribution and the model outputs. In summary, the probe accuracy is 0.64, and the PI between the probes' transformed distribution and the labels is 2.47 vs. 2.58 for the actual model. The entropy (in bits) between the probe outputs and model predictions is 0.27, indicating that most of the relevant behavior is explained by using the probe.

I.1 Logits For ASCAD with Classes

In Figure 15, we show the median logits for traces belonging to classes Y_i. As we can see, the logits corresponding to the expected points in Y_i are always the main peaks.

Figure 16 shows how logits change from epoch 12 to epoch 25. When we analyze using only `S-box` inputs, we see that the logit values are significantly higher before the accuracies for output bits are increased. This is explained by the fact that each of these cases combines four plots (vertically) in Figure 15. Concretely, as for each trace in Figure 16, we combine traces that belong to 4 different classes of the output bits, we expect the logits for each index that belongs to $p \oplus k \mod 4 \equiv i$ to only be high for 1/4 traces, resulting in lower medians. Note that mean values do not show this same trend, as the increase in the Y_i class compensated for this decrease.

To verify that the results in Figure 15 are not an artifact of selecting traces, we visualize the same analysis for bits 2 and 3 in Figure 17. Clearly, the output values are significantly lower than for correct bits, indicating that these bits are (mostly) not being used by the model.

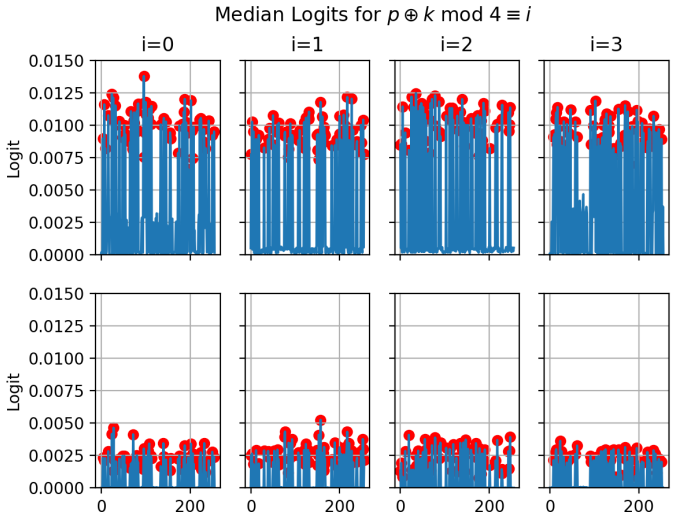

Figure 16: Median logits for traces belonging to varying classes of 2 LSBs of S-box input for epoch 12 (top) and 25 (bottom).

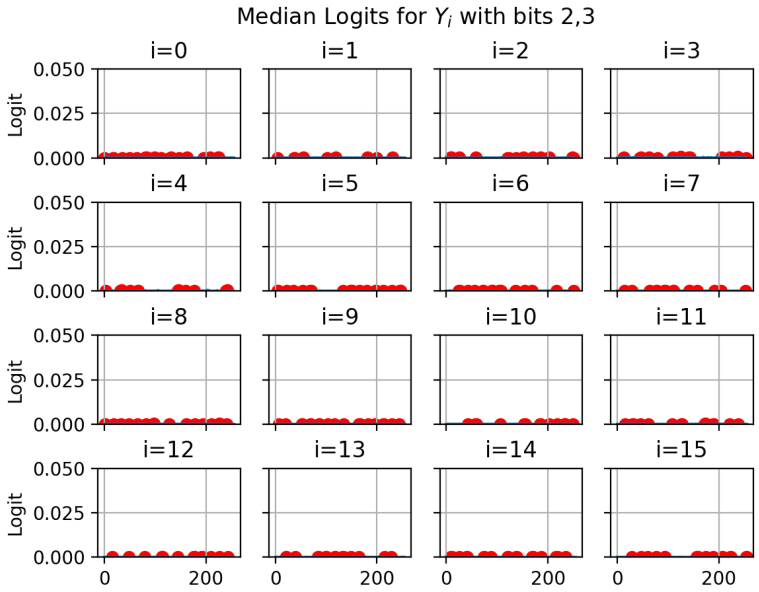

Figure 17: Median logits for traces belonging to varying Y_i for bits 2 and 3. The red dots indicate indices in the respective Y_i.

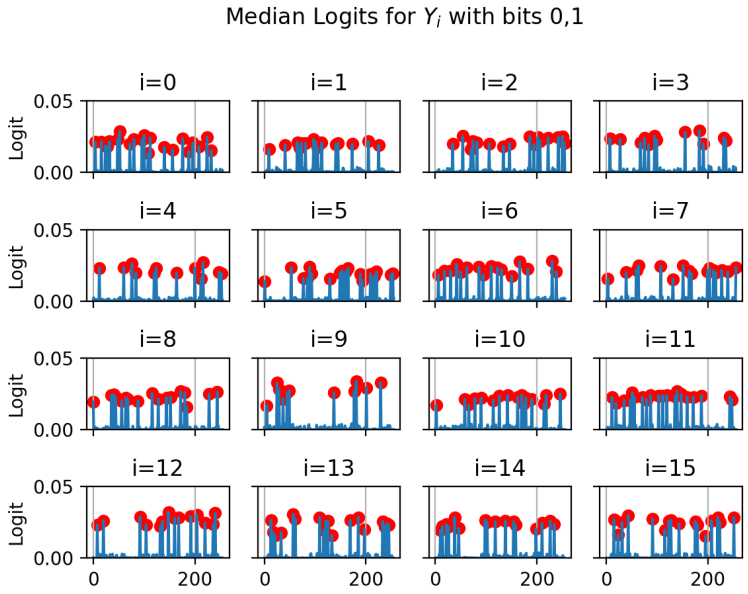

Figure 18: Median logits for traces belonging to varying Y_i classes for CNN model. The red dots indicate indices in the respective Y_i.

NeurIPS Paper Checklist

1. **Claims**

   Question: Do the main claims made in the abstract and introduction accurately reflect the paper's contributions and scope?

   Answer: [Yes]

   Justification: The main claims are supported by experiments against several targets. More speculative claims about implications and generalization are discussed.

   Guidelines:

   - The answer NA means that the abstract and introduction do not include the claims made in the paper.
   - The abstract and/or introduction should clearly state the claims made, including the contributions made in the paper and important assumptions and limitations. A No or NA answer to this question will not be perceived well by the reviewers.
   - The claims made should match theoretical and experimental results, and reflect how much the results can be expected to generalize to other settings.
   - It is fine to include aspirational goals as motivation as long as it is clear that these goals are not attained by the paper.

2. **Limitations**

   Question: Does the paper discuss the limitations of the work performed by the authors?

   Answer: [Yes]

   Justification: Limitations when generalizing to different models and targets are discussed in Section 5. The setting and security assumptions are discussed in the introduction and more concretely at the start of Section 3.

   Guidelines:

   - The answer NA means that the paper has no limitation while the answer No means that the paper has limitations, but those are not discussed in the paper.
   - The authors are encouraged to create a separate "Limitations" section in their paper.

- The paper should point out any strong assumptions and how robust the results are to violations of these assumptions (e.g., independence assumptions, noiseless settings, model well-specification, asymptotic approximations only holding locally). The authors should reflect on how these assumptions might be violated in practice and what the implications would be.
- The authors should reflect on the scope of the claims made, e.g., if the approach was only tested on a few datasets or with a few runs. In general, empirical results often depend on implicit assumptions, which should be articulated.
- The authors should reflect on the factors that influence the performance of the approach. For example, a facial recognition algorithm may perform poorly when image resolution is low or images are taken in low lighting. Or a speech-to-text system might not be used reliably to provide closed captions for online lectures because it fails to handle technical jargon.
- The authors should discuss the computational efficiency of the proposed algorithms and how they scale with dataset size.
- If applicable, the authors should discuss possible limitations of their approach to address problems of privacy and fairness.
- While the authors might fear that complete honesty about limitations might be used by reviewers as grounds for rejection, a worse outcome might be that reviewers discover limitations that aren't acknowledged in the paper. The authors should use their best judgment and recognize that individual actions in favor of transparency play an important role in developing norms that preserve the integrity of the community. Reviewers will be specifically instructed to not penalize honesty concerning limitations.

3. **Theory assumptions and proofs**

   Question: For each theoretical result, does the paper provide the full set of assumptions and a complete (and correct) proof?

   Answer: [NA]

   Justification: The paper does not include theoretical results.

   Guidelines:

   - The answer NA means that the paper does not include theoretical results.
   - All the theorems, formulas, and proofs in the paper should be numbered and cross-referenced.
   - All assumptions should be clearly stated or referenced in the statement of any theorems.
   - The proofs can either appear in the main paper or the supplemental material, but if they appear in the supplemental material, the authors are encouraged to provide a short proof sketch to provide intuition.
   - Inversely, any informal proof provided in the core of the paper should be complemented by formal proofs provided in appendix or supplemental material.
   - Theorems and Lemmas that the proof relies upon should be properly referenced.

4. **Experimental result reproducibility**

   Question: Does the paper fully disclose all the information needed to reproduce the main experimental results of the paper to the extent that it affects the main claims and/or conclusions of the paper (regardless of whether the code and data are provided or not)?

   Answer: [Yes]

   Justification: The (training recipes for) models are described in Appendix C and datasets used in the paper are public. The methods and analyses are described in the paper. Code is also provided with scripts to simplify reproduction.

   Guidelines:

   - The answer NA means that the paper does not include experiments.
   - If the paper includes experiments, a No answer to this question will not be perceived well by the reviewers: Making the paper reproducible is important, regardless of whether the code and data are provided or not.

- If the contribution is a dataset and/or model, the authors should describe the steps taken to make their results reproducible or verifiable.
- Depending on the contribution, reproducibility can be accomplished in various ways. For example, if the contribution is a novel architecture, describing the architecture fully might suffice, or if the contribution is a specific model and empirical evaluation, it may be necessary to either make it possible for others to replicate the model with the same dataset, or provide access to the model. In general. releasing code and data is often one good way to accomplish this, but reproducibility can also be provided via detailed instructions for how to replicate the results, access to a hosted model (e.g., in the case of a large language model), releasing of a model checkpoint, or other means that are appropriate to the research performed.
- While NeurIPS does not require releasing code, the conference does require all submissions to provide some reasonable avenue for reproducibility, which may depend on the nature of the contribution. For example
  (a) If the contribution is primarily a new algorithm, the paper should make it clear how to reproduce that algorithm.
  (b) If the contribution is primarily a new model architecture, the paper should describe the architecture clearly and fully.
  (c) If the contribution is a new model (e.g., a large language model), then there should either be a way to access this model for reproducing the results or a way to reproduce the model (e.g., with an open-source dataset or instructions for how to construct the dataset).
  (d) We recognize that reproducibility may be tricky in some cases, in which case authors are welcome to describe the particular way they provide for reproducibility. In the case of closed-source models, it may be that access to the model is limited in some way (e.g., to registered users), but it should be possible for other researchers to have some path to reproducing or verifying the results.

5. **Open access to data and code**

   Question: Does the paper provide open access to the data and code, with sufficient instructions to faithfully reproduce the main experimental results, as described in supplemental material?

   Answer: [Yes]

   Justification: Code is included, there are scripts to download and extract the used datasets from raw traces. We also provided links to download model checkpoints used and extracted datasets to simplify reproduction.

   Guidelines:

   - The answer NA means that paper does not include experiments requiring code.
   - Please see the NeurIPS code and data submission guidelines (`https://nips.cc/public/guides/CodeSubmissionPolicy`) for more details.
   - While we encourage the release of code and data, we understand that this might not be possible, so "No" is an acceptable answer. Papers cannot be rejected simply for not including code, unless this is central to the contribution (e.g., for a new open-source benchmark).
   - The instructions should contain the exact command and environment needed to run to reproduce the results. See the NeurIPS code and data submission guidelines (`https://nips.cc/public/guides/CodeSubmissionPolicy`) for more details.
   - The authors should provide instructions on data access and preparation, including how to access the raw data, preprocessed data, intermediate data, and generated data, etc.
   - The authors should provide scripts to reproduce all experimental results for the new proposed method and baselines. If only a subset of experiments are reproducible, they should state which ones are omitted from the script and why.
   - At submission time, to preserve anonymity, the authors should release anonymized versions (if applicable).
   - Providing as much information as possible in supplemental material (appended to the paper) is recommended, but including URLs to data and code is permitted.

6. **Experimental setting/details**

   Question: Does the paper specify all the training and test details (e.g., data splits, hyperparameters, how they were chosen, type of optimizer, etc.) necessary to understand the results?

   Answer: [Yes]

   Justification: The (training recipes for) models are described in Appendix C (and based on results in [35]) and the train/test splits are standard for the used datasets.

   Guidelines:

   - The answer NA means that the paper does not include experiments.
   - The experimental setting should be presented in the core of the paper to a level of detail that is necessary to appreciate the results and make sense of them.
   - The full details can be provided either with the code, in appendix, or as supplemental material.

7. **Experiment statistical significance**

   Question: Does the paper report error bars suitably and correctly defined or other appropriate information about the statistical significance of the experiments?

   Answer: [No]

   Justification: The experiments are reverse engineering specific models from previous works..

   Guidelines:

   - The answer NA means that the paper does not include experiments.
   - The authors should answer "Yes" if the results are accompanied by error bars, confidence intervals, or statistical significance tests, at least for the experiments that support the main claims of the paper.
   - The factors of variability that the error bars are capturing should be clearly stated (for example, train/test split, initialization, random drawing of some parameter, or overall run with given experimental conditions).
   - The method for calculating the error bars should be explained (closed form formula, call to a library function, bootstrap, etc.)
   - The assumptions made should be given (e.g., Normally distributed errors).
   - It should be clear whether the error bar is the standard deviation or the standard error of the mean.
   - It is OK to report 1-sigma error bars, but one should state it. The authors should preferably report a 2-sigma error bar than state that they have a 96% CI, if the hypothesis of Normality of errors is not verified.
   - For asymmetric distributions, the authors should be careful not to show in tables or figures symmetric error bars that would yield results that are out of range (e.g. negative error rates).
   - If error bars are reported in tables or plots, The authors should explain in the text how they were calculated and reference the corresponding figures or tables in the text.

8. **Experiments compute resources**

   Question: For each experiment, does the paper provide sufficient information on the computer resources (type of compute workers, memory, time of execution) needed to reproduce the experiments?

   Answer: [Yes]

   Justification: The amount of compute and resources is described in Appendix D

   Guidelines:

   - The answer NA means that the paper does not include experiments.
   - The paper should indicate the type of compute workers CPU or GPU, internal cluster, or cloud provider, including relevant memory and storage.
   - The paper should provide the amount of compute required for each of the individual experimental runs as well as estimate the total compute.

- The paper should disclose whether the full research project required more compute than the experiments reported in the paper (e.g., preliminary or failed experiments that didn't make it into the paper).

9. **Code of ethics**

   Question: Does the research conducted in the paper conform, in every respect, with the NeurIPS Code of Ethics `https://neurips.cc/public/EthicsGuidelines`?

   Answer: [Yes]

   Justification: The paper works on interpreting models in DLSCA. Techniques to extract mask values could potentially be used to improve attacks and broader improvements to DLSCA can improve practical attacks. However, the main purpose is to improve evaluation procedures which should improve the (confidence in the) security of implementations against such attacks.

   Guidelines:

   - The answer NA means that the authors have not reviewed the NeurIPS Code of Ethics.
   - If the authors answer No, they should explain the special circumstances that require a deviation from the Code of Ethics.
   - The authors should make sure to preserve anonymity (e.g., if there is a special consideration due to laws or regulations in their jurisdiction).

10. **Broader impacts**

    Question: Does the paper discuss both potential positive societal impacts and negative societal impacts of the work performed?

    Answer: [NA]

    Justification: The paper works on advancing deep learning-based SCA which is dual-use but mainly used in evaluation procedures for testing whether implementations are sufficiently secure. The impacts of this specific work on the SCA domain are discussed in Section 5.

    Guidelines:

    - The answer NA means that there is no societal impact of the work performed.
    - If the authors answer NA or No, they should explain why their work has no societal impact or why the paper does not address societal impact.
    - Examples of negative societal impacts include potential malicious or unintended uses (e.g., disinformation, generating fake profiles, surveillance), fairness considerations (e.g., deployment of technologies that could make decisions that unfairly impact specific groups), privacy considerations, and security considerations.
    - The conference expects that many papers will be foundational research and not tied to particular applications, let alone deployments. However, if there is a direct path to any negative applications, the authors should point it out. For example, it is legitimate to point out that an improvement in the quality of generative models could be used to generate deepfakes for disinformation. On the other hand, it is not needed to point out that a generic algorithm for optimizing neural networks could enable people to train models that generate Deepfakes faster.
    - The authors should consider possible harms that could arise when the technology is being used as intended and functioning correctly, harms that could arise when the technology is being used as intended but gives incorrect results, and harms following from (intentional or unintentional) misuse of the technology.
    - If there are negative societal impacts, the authors could also discuss possible mitigation strategies (e.g., gated release of models, providing defenses in addition to attacks, mechanisms for monitoring misuse, mechanisms to monitor how a system learns from feedback over time, improving the efficiency and accessibility of ML).

11. **Safeguards**

    Question: Does the paper describe safeguards that have been put in place for responsible release of data or models that have a high risk for misuse (e.g., pretrained language models, image generators, or scraped datasets)?

    Answer: [NA]

Justification: The paper focuses interpreting models that break specific public implementations from previous works. Therefore materials in this work pose no such risks.

Guidelines:

- The answer NA means that the paper poses no such risks.
- Released models that have a high risk for misuse or dual-use should be released with necessary safeguards to allow for controlled use of the model, for example by requiring that users adhere to usage guidelines or restrictions to access the model or implementing safety filters.
- Datasets that have been scraped from the Internet could pose safety risks. The authors should describe how they avoided releasing unsafe images.
- We recognize that providing effective safeguards is challenging, and many papers do not require this, but we encourage authors to take this into account and make a best faith effort.

12. **Licenses for existing assets**

    Question: Are the creators or original owners of assets (e.g., code, data, models), used in the paper, properly credited and are the license and terms of use explicitly mentioned and properly respected?

    Answer: [Yes]

    Justification: All of the used datasets are publicly available and credited.

    Guidelines:

    - The answer NA means that the paper does not use existing assets.
    - The authors should cite the original paper that produced the code package or dataset.
    - The authors should state which version of the asset is used and, if possible, include a URL.
    - The name of the license (e.g., CC-BY 4.0) should be included for each asset.
    - For scraped data from a particular source (e.g., website), the copyright and terms of service of that source should be provided.
    - If assets are released, the license, copyright information, and terms of use in the package should be provided. For popular datasets, `paperswithcode.com/datasets` has curated licenses for some datasets. Their licensing guide can help determine the license of a dataset.
    - For existing datasets that are re-packaged, both the original license and the license of the derived asset (if it has changed) should be provided.
    - If this information is not available online, the authors are encouraged to reach out to the asset's creators.

13. **New assets**

    Question: Are new assets introduced in the paper well documented and is the documentation provided alongside the assets?

    Answer: [NA]

    Justification: The paper provides no new assets.

    Guidelines:

    - The answer NA means that the paper does not release new assets.

14. **Crowdsourcing and research with human subjects**

    Question: For crowdsourcing experiments and research with human subjects, does the paper include the full text of instructions given to participants and screenshots, if applicable, as well as details about compensation (if any)?

    Answer: [NA]

    Justification: The paper does not involve crowdsourcing nor research with human subjects

    Guidelines:

    - The answer NA means that the paper does not involve crowdsourcing nor research with human subjects.

- Including this information in the supplemental material is fine, but if the main contribution of the paper involves human subjects, then as much detail as possible should be included in the main paper.
- According to the NeurIPS Code of Ethics, workers involved in data collection, curation, or other labor should be paid at least the minimum wage in the country of the data collector.

15. **Institutional review board (IRB) approvals or equivalent for research with human subjects**

    Question: Does the paper describe potential risks incurred by study participants, whether such risks were disclosed to the subjects, and whether Institutional Review Board (IRB) approvals (or an equivalent approval/review based on the requirements of your country or institution) were obtained?

    Answer: [NA]

    Justification: The paper does not involve crowdsourcing nor research with human subjects

    Guidelines:

    - The answer NA means that the paper does not involve crowdsourcing nor research with human subjects.
    - Depending on the country in which research is conducted, IRB approval (or equivalent) may be required for any human subjects research. If you obtained IRB approval, you should clearly state this in the paper.
    - We recognize that the procedures for this may vary significantly between institutions and locations, and we expect authors to adhere to the NeurIPS Code of Ethics and the guidelines for their institution.
    - For initial submissions, do not include any information that would break anonymity (if applicable), such as the institution conducting the review.

16. **Declaration of LLM usage**

    Question: Does the paper describe the usage of LLMs if it is an important, original, or non-standard component of the core methods in this research? Note that if the LLM is used only for writing, editing, or formatting purposes and does not impact the core methodology, scientific rigorousness, or originality of the research, declaration is not required.

    Answer: [NA]

    Justification: The core method development in this research does not involve LLMs as any important, original, or non-standard components.

    Guidelines:

    - The answer NA means that the core method development in this research does not involve LLMs as any important, original, or non-standard components.
    - Please refer to our LLM policy (`https://neurips.cc/Conferences/2025/LLM`) for what should or should not be described.